



## MICROSTRUCTURE AND THERMAL ANALYSIS OF BRAKE PADS DEVELOPED FROM ASBESTOS-FREE MATERIALS

J. Abutu<sup>1\*</sup>, S. A. Lawal<sup>2</sup>, R. A. Lafia-Araga<sup>3</sup>, M. B. Ndaliman<sup>2</sup> and M. A. Oluleye<sup>4</sup>

<sup>1</sup>Department of Mechanical Engineering, Taraba State University, Jalingo-Nigeria

<sup>2</sup>Department of Mechanical Engineering, Federal University of Technology, Minna-Nigeria

<sup>3</sup>Department of Chemistry, Federal University of Technology, Minna-Nigeria

<sup>4</sup>Department of Mechanical Engineering, Faculty of Engineering, Ekiti State University, Ado-Ekiti

\*Corresponding author's email address: [abutu.joseph@tsuniversity.edu.ng](mailto:abutu.joseph@tsuniversity.edu.ng)

### ARTICLE INFORMATION

Submitted 08 Feb., 2019  
Revised 07 March, 2020  
Accepted 10 March, 2020

### Keywords:

Brake pad;  
microstructure;  
thermogravimetric  
analysis; seashells; coconut  
shells.

### ABSTRACT

This study was conducted on developed asbestos-free brake pad using coconut shell and seashell as fillers. The use of hazardous reinforcement like asbestos fiber in friction materials is being avoided because of its carcinogenic effects. Rule of mixture technique was utilized during sample formulation and a weight percent of 52% filler material, 5% friction modifier, 8% abrasive and 35% binder were utilized for production. A multi-response optimization technique (grey relational analysis) was used to obtain an optimal process parameter of moulding pressure (14 MPa), moulding temperature (140°C), curing time (8 minutes) and heat treatment time (5 hours) for coconut shell-filled brake pad and moulding pressure (14 MPa), moulding temperature (160°C), curing time (12 minutes) and heat treatment time (1 hour) for seashell-filled brake pad. Thermal analysis of commercial and optimized samples shows that the commercial brake pads possesses a better thermal stability compared to the optimized formulated brake pad samples with the coconut shell-filled samples showing the least thermal resistance. Also, microstructure analysis of the impact fractured surfaces of the commercial, seashell and coconut shell-filled brake pad was conducted using scanning electron microscope (SEM). The results revealed that compare the commercial and seashell-filled samples, there were more uniform distribution of the resin in the coconut shell-filled composite leading to an improved bonding and closer inter- packing distance between its constituent particles and the epoxy resin. It was also revealed that the commercial brake pad possessed a higher thermal stability as the components were not noticeably degraded at temperatures at which the coconut shell and the seashell filled brake pads showed appreciable degradation.

© 2020 Faculty of Engineering, University of Maiduguri, Nigeria. All rights reserved.

## 1.0 Introduction

Friction materials are heterogeneous substances composed of different constituents. Each constituent element performs its own functions. These include improvement in frictional properties at low and high temperature, increase in strength, reduction in noise, prolonged life, rigidity and reduced porosity (Natarajan et al., 2012). Changes in the weight percentage or composition may lead to the alteration of the thermal, morphological, chemical, physical and mechanical properties of the developed brake pad materials (Jang et al., 2004, Mutlu et al., 2005, Cho et al., 2005, Zaharudin et al., 2011). Early researchers have concluded that no simple relationship exist between properties of frictional materials (Talib et al., 2012, Tanaka et al., 1973). Industrial brake pads are usually made up of large number of constituents such as fibres, metallic chips, solid lubricants, ceramic particles, minerals, and elastomers in a matrix material like phenolic resin. The use of antimony in brake pads was investigated by Ole-Von et al. (2005) and it was found that the use of antimony in brake pad should be suspended as it posed a human cancer risk due to considerable antimony concentrations in the material.

The use of agricultural wastes is also rising as inexpensive and new materials in brake pads development, with environmental acceptability and commercial viability (Bhaskar and Vinay, 2013). Cyras et al. (2001) reported that among the different kinds of agricultural products investigated, lignocellulose fillers such as coconut shells are most times seen as attractive

materials to be utilised as fillers due to its excellent properties. Microstructure and thermal examination of newly developed formulations are required to assess their performance using microscopy and thermal stability testing with the aim of ascertaining that the developed brake pad meets the minimum requirements of its intended use (Talib et al., 2012). In a related study, Aigbodion et al. (2010) developed an asbestos-free brake pad using sugar cane bagasse as reinforcement and studied the microstructure and thermal resistance. The authors reported that there was more uniform distribution of the bagasse within the resin, as the particles size of the bagasse decreased. Ikpambese et al. (2014) investigated the microstructure of worn surfaces of palm kernel fibre-reinforce pads. The result of the microstructural examination revealed that worn surfaces were characterized by abrasion wear, where the asperities were ploughed thereby exposing the white region of palm kernel fibres, thus increasing the smoothness of the friction materials. Yawas et al. (2016) also used scanning electron microscope to study the distribution of periwinkle shell particle in phenolic resin using different sieve sizes. The results showed that the microstructures of samples revealed a homogeneous distribution as the sieve sizes decreased. Similarly, Ruzaidi et al. (2011) studied the microstructure of fractured surfaces of palm ash and PCB waste-containing friction material. Overall observation shows the mixture of the brake pad materials were well dispersed even though there are some traces of pores due to the different particle size of each mixture. Lawal et al. (2016) also studied the thermal degradation behaviour of rubber-scrap filled brake pad. The results indicate that the formulated sample degraded between 149.9 and 478.4 °C, with peak degradation at temperature 394.8 °C.

In addition, the thermal decomposition of calcium carbonate ( $\text{CaCO}_3$ ) and seashells were studied by Islam et al. (2013) and Nurfatihah et al. (2015) respectively and the results showed that the decomposition pattern revealed two distinct phases. The first phase began with a minimum loss in weight while the second phase started at 580°C and stopped at 815°C. Andrzej et al. (2010) studied the thermal stability of soft wood fiber, coconut shell and barley husk filled polypropylene composite and revealed that the total moisture content by fiber was removed before 150°C while the decomposition temperature for coconut shell, barley husk and soft wood fiber were at 195°C, 235°C and 245°C respectively. Also, the thermal decomposition of calcium carbonate in cockle shell was also studied by Mustakimah et al. (2012) using thermogravimetric analyzer and reported that as the temperatures increased from 700-900°C, a quick change in weights of the samples occurred as the volatile material attempted to escape at the start of decomposition process. The thermal decomposition kinetics of epoxy resins in nitrogen-oxygen environment was also studied by Chen et al. (1997) using a heating conditions of 20, 10, 5, and 2 K/min and revealed that under pure nitrogen atmosphere, only one peak temperature (459°C) was found. Also, Yasmin and Daniel (2004) studied the thermal stability of graphite/epoxy composite and revealed that a very high thermal stability was exhibited by pure graphite with only 1.6% of the entire weight of graphite lost at a temperature of 800°C. The authors concluded that the inclusion of the graphite in composite production improved its thermal stability. Therefore, in this study, two material (seashells and coconut shells) combined separately with other additives (graphite and alumina) were used to develop pads using powder metallurgy technique employing statistical method such as grey relational analysis (GRA) and response surface methodology experimental design. The morphology and thermal behaviour of the developed materials were also investigated with the aim of comparing the microstructure and thermal stability of the various constituents of the developed and commercial brake pad sample.

## 2. Materials and Methods

### 2.1 Materials

Aluminium oxide (Lot. No. 44100; Cat. No. 34143) obtained from a commercial chemical shop in Onitsha, Anambra State, Nigeria. This material was included to serve as an abrasive. Graphite powder (friction modifier) was sourced from used 1.5 volt TIGER head dry cell batteries. Epoxy resin (Epoblock, FIP Chemicals) was used together with a hardener (Sikadur 42T; Sika Corporation U.S.A) and were obtained from a chemical store located in Onitsha, Anambra State, Nigeria. Coconut shells were obtained from a coconut trader in a Sabon-Tasha market in Kaduna, Nigeria while seashells (the shells of sea snails) were collected from a local

seafood vendor in Lagos bar beach, Lagos, Nigeria. Seashells and coconut shells (Figure 1) were used as fillers.



Figure 1: Fillers

## 2.2 Methods

### 2.2.1 Materials preparation

As adopted by Ikpambese et al. (2014) and Abutu et al. (2018), the method involved in the preparation of the fillers (coconut shell and seashell) as well as graphite powder included washing of sourced materials, followed by cleaning with dried cloth and thereafter drying in an air circulating oven of 150°C operating temperature. Further preparation process involved crushing of the oven-dried filler materials with pestle and mortar as well as grinding using a grinder and finally sieving using a 10 µm.

### 2.2.2 Formulation of Brake pad

In this study, Rule of mixture (ROM) was utilized in the formulation of the brake pads. This technique will help predict the brake pads properties and also provide information about the percentage composition of each constituent material in the developed brake pads. As suggested by Ikpambese et al. (2014), sample formulation was based on 176g standard weight of commercial brake pad. Eqns. 1 and 2 were utilized in the calculation of volume fraction (f) and theoretical densities (d) of the brake pads respectively (Askeland, 1985).

$$\text{Volume fraction}(f_i) = \frac{p_i}{d_i} \div \sum \frac{p_j}{d_j} \quad (1)$$

$$d_{\text{composite}} = d_f f_f + d_a f_a + d_{fm} f_{fm} + d_b f_b \quad (2)$$

where:  $p_j$  and  $p_i$  is the weight percent of the total and individual constituent respectively,  $f_i$  is the individual volume fraction.  $d_j$  and  $d_i$  are densities of total and the individual constituents respectively.  $d_{\text{composite}}$  is the theoretical densities of the seashell or coconut shell filled composite,  $d_f$  and  $f_f$  are the density and volume fraction of the filler,  $d_a$  and  $f_a$  are the density and volume fraction of the abrasive,  $d_{fm}$  and  $f_{fm}$  are the density and volume fraction of the friction modifier while  $d_b$  and  $f_b$  are the density and volume fraction of the binder.

### 2.2.3 Experimental Design and Grey Relational Analysis

In this study, central composite design (CCD) via response surface methodology (RSM) and Grey relational analysis (GRA) was used to obtain optimal brake pad composite. This experimental design was built using Minitab 17 software in accordance with standard RSM's L27 (2)<sup>4</sup> where MT (molding temperature), MP (molding pressure), CT (curing time) and HTT (heat treatment time) were chosen as the process parameters. The data obtained from mechanical and tribological examination of samples produced using CCD experimental design were used to conduct grey relational analysis (GRA) with the aim of obtaining optimal process parameters that will give the multi-response optimal performance in terms of its microstructure and thermal behaviour.

Grey relational grades (GR-grades) represent the average of grey relational coefficient (GRC) of individual responses investigated. Abutu et al. (2018) reported that grey relational coefficient can be calculated using Eqn. 3.

$$\eta(k_{oj}, k_{ij}) = \frac{\omega \Delta_{\max} + \Delta_{\min}}{\omega \Delta_{\max} + \Delta_{ij}} \quad (i = 1, 2, \dots, 27 \text{ and } j = 1, 2, \dots, 27) \quad (3)$$

where:  $\eta(k_{0j}, k_{ij})$  is the GRC between  $k_{ij}$  and  $k_{0j}$ ,  $\Delta_{ij} = k_{0j} - k_{ij}$ ,  $\Delta_{min} = \min(\Delta_{ij}, i = 1, 2, \dots, m; j = 1, 2, \dots, n)$ ,  $\omega$  is the distinguishing coefficient,  $\omega \in [0, 1]$  and  $\Delta_{max} = \max(\Delta_{ij}, i = 1, 2, \dots, 27; j = 1, 2, \dots, 27)$

$\omega$  was introduced in order to modify (compress or expand) the range of GRC. Yiyo et al. (2008) reported that,  $\omega = 0.5$ ,  $\Delta_{max} = 1$  and  $\Delta_{min} = 0$ .

### 2.2.4 Production of Brake Pad Samples using optimized values

Production of optimized samples was carried out on a compression moulding machine (Model: 0577-86365889, Wenzhou Zhiguang Shoe-Making Machine Co. Ltd, China) using standard procedure specified by Chemiplastica (2010) and Abutu et al. (2019).

### 2.2.5 Thermogravimetric Analysis (TGA)

Thermogravimetric analysis was conducted on between 10 to 20 mg samples on Platinum pans using Perkin Elmer Pyris TGA 1, (USA), at a heating rate of 10.00°C/min from 50 to 950°C in nitrogen atmosphere at a flow rate of 20 mL/min. The weight change with temperature was analysed using the Pyris software. Peak degradation temperature ( $T_p$ ) was recorded as the temperature at which maximum degradation of the material occurred. This represents the peak of the derivative weight change with time.

### 2.2.6 Microstructural Analysis

Impact fractured surfaces of the optimized and commercial samples were observed using scanning electron microscope (TESCAN Vegan III XMU Q150 TE, USA), operating at an accelerating voltage of 10 kV after gold sputter coating at the Characterisation Laboratory of Shehu Musa Ya'radua University, Kastina, Kastina State, Nigeria. This result was achieved by clamping the specimen on the mechanical part of the microscope and using the adjustment knob to adjust the lens of microscope. Immediately a clear image was observed at the specified magnification, the process was stopped, and the image captured on the computer connected to it with the aid of software was saved.

## 3. Results and Discussion

### 3.1 Design Matrix and Grey Relational Analysis

Table 1 shows the process factor levels, while Table 2 shows the experimental design matrix for RSM -CCD and the GR- grades for seashell and coconut shell-filled brake pads obtained from GRA.

Table 1: Process Factor Levels

| Factors  | Level 1 | Level 2 | Level 3 | Level 4 | Level 5 |
|----------|---------|---------|---------|---------|---------|
| HTT (hr) | 2.0     | 4.0     | 3       | 1       | 5       |
| CT (min) | 6.0     | 10.0    | 8       | 4       | 12      |
| MT (°C)  | 120     | 160     | 140     | 100     | 180     |
| MP (MPa) | 12      | 16      | 14      | 10      | 18      |

Table 2: Experimental Matrix for RSM -CCD and GR-Grades

| Ru<br>n | Experimental Design |                |            |             | GR-Grade                  |                                |
|---------|---------------------|----------------|------------|-------------|---------------------------|--------------------------------|
|         | HTT<br>(hour)       | CT<br>(minute) | MT<br>(°C) | MP<br>(MPa) | Seashell-Filled<br>sample | Coconut Shell-Filled<br>sample |
| 1       | 2                   | 6              | 120        | 12          | 0.4242                    | 0.6346                         |
| 2       | 2                   | 6              | 120        | 16          | 0.4521                    | 0.6031                         |
| 3       | 2                   | 6              | 160        | 12          | 0.5588                    | 0.6731                         |
| 4       | 2                   | 6              | 160        | 16          | 0.4669                    | 0.5305                         |
| 5       | 2                   | 10             | 120        | 12          | 0.4707                    | 0.8122                         |
| 6       | 2                   | 10             | 120        | 16          | 0.4850                    | 0.5197                         |
| 7       | 2                   | 10             | 160        | 12          | 0.7349                    | 0.5588                         |
| 8       | 2                   | 10             | 160        | 16          | 0.4780                    | 0.5739                         |
| 9       | 4                   | 6              | 120        | 12          | 0.5271                    | 0.4421                         |
| 10      | 4                   | 6              | 120        | 16          | 0.5647                    | 0.6392                         |
| 11      | 4                   | 6              | 160        | 12          | 0.5748                    | 0.5592                         |

|    |   |    |     |    |        |        |
|----|---|----|-----|----|--------|--------|
| 12 | 4 | 6  | 160 | 16 | 0.6528 | 0.4211 |
| 13 | 4 | 10 | 120 | 12 | 0.4531 | 0.7152 |
| 14 | 4 | 10 | 120 | 16 | 0.5049 | 0.6085 |
| 15 | 4 | 10 | 160 | 12 | 0.7076 | 0.5979 |
| 16 | 4 | 10 | 160 | 16 | 0.8833 | 0.6630 |
| 17 | 3 | 8  | 140 | 10 | 0.5967 | 0.5481 |
| 18 | 3 | 8  | 140 | 18 | 0.3976 | 0.5689 |
| 19 | 3 | 8  | 100 | 14 | 0.6236 | 0.6209 |
| 20 | 3 | 8  | 180 | 14 | 0.4411 | 0.5622 |
| 21 | 3 | 4  | 140 | 14 | 0.5040 | 0.4482 |
| 22 | 3 | 12 | 140 | 14 | 0.6596 | 0.5577 |
| 23 | 1 | 8  | 140 | 14 | 0.8748 | 0.6360 |
| 24 | 5 | 8  | 140 | 14 | 0.6077 | 0.7403 |
| 25 | 3 | 8  | 140 | 14 | 0.5987 | 0.7193 |
| 26 | 3 | 8  | 140 | 14 | 0.6288 | 0.7375 |
| 27 | 3 | 8  | 140 | 14 | 0.6086 | 0.7355 |

The resulting process parameters factor effects for seashell and coconut shell-filled samples are shown in Tables 3 and 4. The values in bold indicates the multi-response optimal level for each process parameters. The main effect plots obtained using Table 3 and 4 are shown in Figure 2 and 3.

Table 3: Factor Effects of Process Parameters (Seashell-Filled Samples)

| Factor | Level 1 | Level 2 | Level 3 | Level 4 | Level 5 |
|--------|---------|---------|---------|---------|---------|
| HTT    | 0.8748  | 0.5088  | 0.5621  | 0.6085  | 0.6077  |
| CT     | 0.5040  | 0.5277  | 0.5975  | 0.5897  | 0.6596  |
| MT     | 0.6236  | 0.4852  | 0.6085  | 0.6321  | 0.4411  |
| MP     | 0.5967  | 0.5564  | 0.6163  | 0.5610  | 0.3976  |

Table 4: Factor Effects of Process Parameters (Coconut Shell-Filled Samples)

| Factor | Level 1 | Level 2 | Level 3 | Level 4  | Level 5 |
|--------|---------|---------|---------|----------|---------|
| HTT    | 0.636   | 0.6132  | 0.6109  | 0.580775 | 0.7403  |
| CT     | 0.4482  | 0.5629  | 0.6521  | 0.63115  | 0.5577  |
| MT     | 0.6209  | 0.6218  | 0.6324  | 0.572188 | 0.5622  |
| MP     | 0.5481  | 0.6241  | 0.6397  | 0.569875 | 0.5689  |

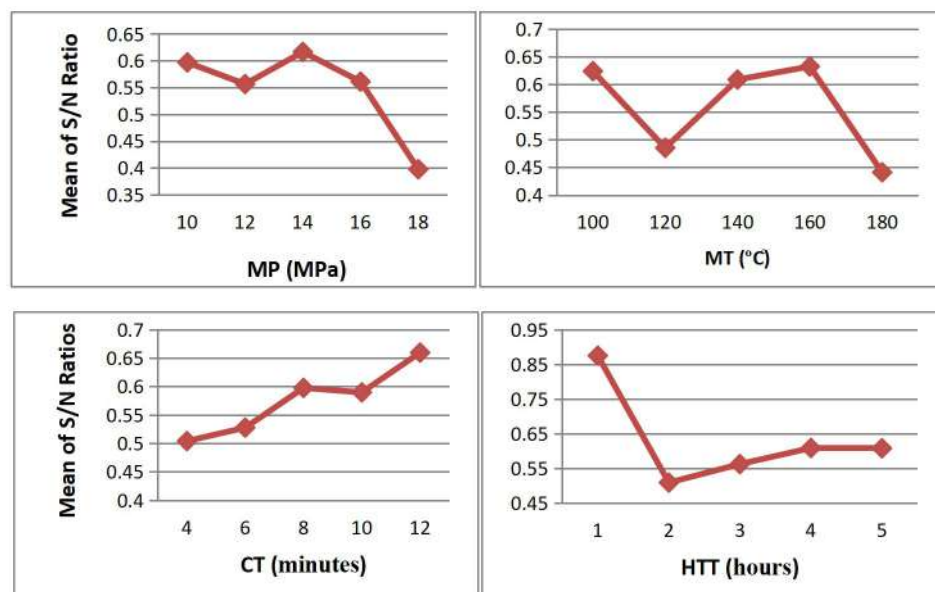


Figure 2: Plots of Factor Effects (Seashell-filled Samples)

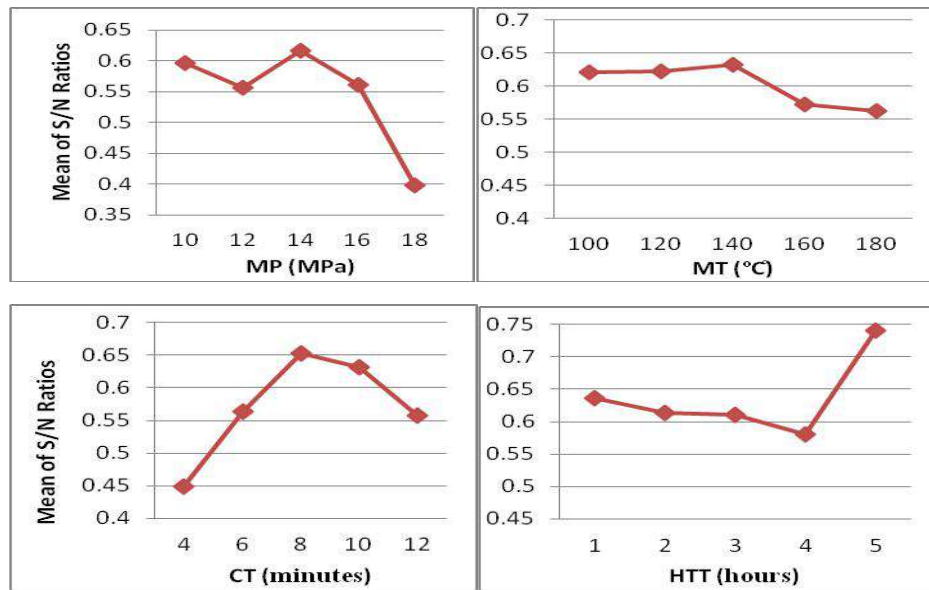


Figure 3: Plots of Factor Effects (Coconut Shell filled Samples)

From Figure 2, it can be observed that the optimum values of seashell-filled brake pad can be obtained using 1 hour heat treatment time, 12 minutes curing time, 160 °C moulding temperature and 14MPa moulding pressure while Figure 3 shows that optimum values of coconut shell filled brake pad samples can be obtained using 5 hours heat treatment time, 8 minutes curing time, 140 °C moulding temperature and 14 MPa moulding pressure. These results are in conformity with earlier work of Dagwa and Ibhadode (2006), who reported HTT (2 hours), CT (8 minutes), MT (160°C) and MP (16.74MPa) as optimal process parameter using palm kernel shells as filler material.

### 3.2 Optimized samples

During the production of the optimized samples, the optimal process parameters obtained using GRA as shown in Figure 2 and 3 were used while the composition of the samples formulated using rule of mixture (Table 5) remained constant throughout the process. As suggested by Abutu et al. (2018), preliminary preparation involved pouring 41.06 g (23.33 %) of the resin into a container followed by the addition of 20.54 g (11.67 %) of hardener (catalyst).

The mixture of hardener and resin were stirred manually in a separate stainless steel bowl until homogenous mixture was observed while mixture of the weighed fillers (shells, friction modifier and abrasive) were also manually stirred in another separate stainless steel bowl. The entire mixture was afterward transferred into a fabricated mould of size 124 x 112 x 10 mm for compression moulding, using the optimized process parameters. The final products (Figure 4) were subjected to further heat treatment using the optimal HTT presented in Figure 2 and 3 with the aid of a hot air oven (150°C).

Table 5: Composition of optimized brake pad sample

| Ingredient                 | Filler (Coconut shell or seashell) | Binder (Epoxy resin) | Binder (Hardener) | Abrasive (Alumina) | Friction modifier (Graphite) |
|----------------------------|------------------------------------|----------------------|-------------------|--------------------|------------------------------|
| Percentage composition (%) | 52                                 | 23.33                | 11.67             | 8                  | 5                            |
| Mass composition (g)       | 91.52                              | 41.06                | 20.54 g           | 14.01              | 8.80                         |

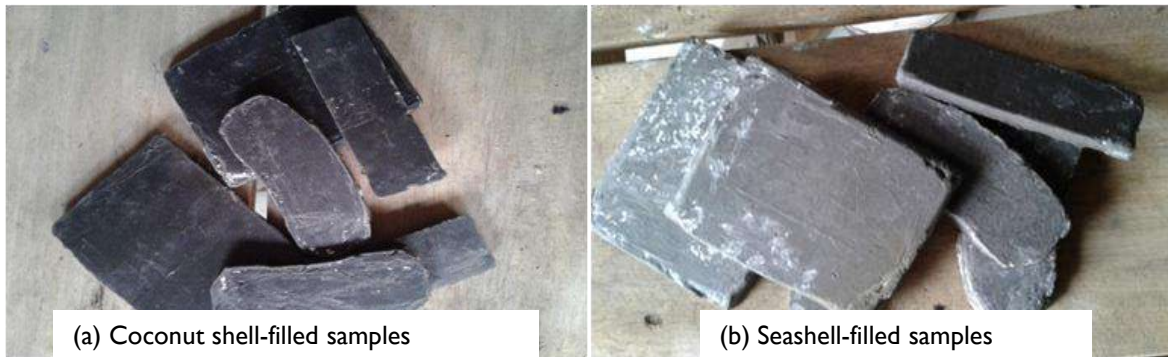


Figure 4: Heat treated optimized samples (a) seashell and (b) coconut shell filled brake pad samples

### 3.3 Thermogravimetric Analysis (TGA)

The results of TGA and derivative thermogravimetric (DTG) analysis for commercial as well as coconut shell and seashell filled brake pads are presented in Figures 5 and 6. Data extracted from these thermograms are presented in Table 6. The temperature range used in this experiment is below the degradation temperature for all the components of the commercial and the seashell brake pads.

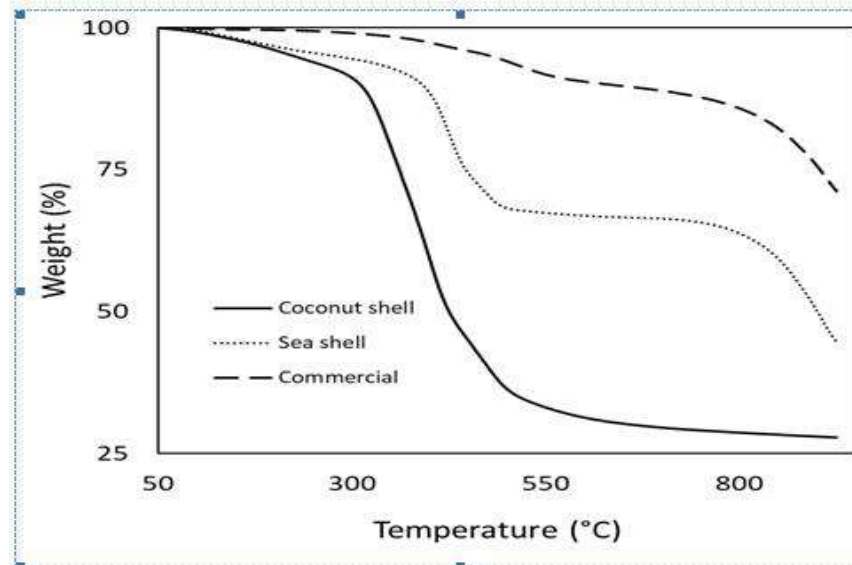


Fig. 5: TGA curves of coconut shell, seashell and commercial brake pad.

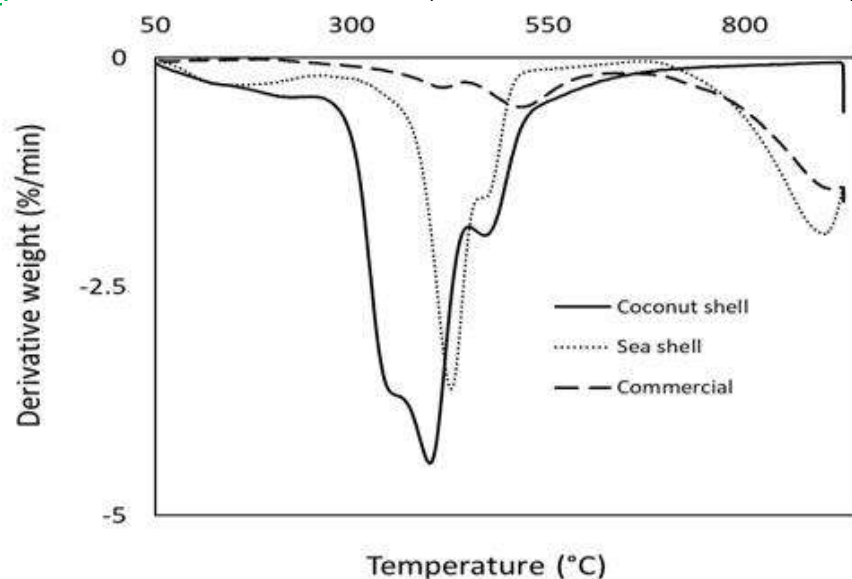


Fig. 6: DTG curves of coconut shell, seashell and commercial brake pad

Table 6: TGA data for coconut, sea shell filled and commercial brake pads

| Sample        | Onset temperature, Tonset 1 (°C) | Onset temperature, Tonset 2 (°C) | Peak degradation temperature, T <sub>p1</sub> (°C) | Peak degradation temperature, T <sub>p2</sub> (°C) | Peak degradation temperature, T <sub>p3</sub> (°C) |
|---------------|----------------------------------|----------------------------------|--|--|--|
| Coconut shell | 308.6                            | None                             | 350.5  | 475.7  | -  |
| Sea shell     | 394.3                            | 806.4                            | 427.1  | 473.1  | 897.6  |
| Commercial    | 400.2                            | 824.1                            | 415.3  | 514.1  | 903.2  |

Due to the fact that there is no concise data relating to the components of the commercial sample, the thermal degradation pattern of only the coconut and seashell filled samples will be discussed. However, a comparison was made with the commercial sample with respect to thermal stability. In addition, from the TGA residue, the commercial samples were found to contain asbestos fibres. This may be responsible for the superior thermal properties of the commercial sample as indicated by the thermal degradation profile of the optimized coconut shell-filled, seashell-filled and commercial sample shown in the TGA and the DTG curves in Figure 5 and 6 respectively. Similar degradation profile was observed for the coconut and the seashell brake pads, although the events occurred at different temperatures. An initial degradation is seen below 250°C. A close observation of this event revealed two overlapping events which occurred between 100 and 150°C. Evaporation of moisture from the samples took place at this stage. Also, another shoulder overlapping with this event up till 250°C could also be seen which may be attributed to the release of volatiles from the samples. This release of volatiles is more pronounced in the coconut shell than in the seashell samples and could be as a result of the extractives present in the coconut shell and the hardener used in the formulation. A small shoulder in the coconut-filled brake pad is also seen at about 350°C. This is attributed to the degradation of hemicelluloses in the coconut shell (Chun et al., 2013a). Hemicellulose has been reported to be the most thermally unstable component of a lignocellulosic material (Chun et al., 2013b). From the coconut shell filled brake pad, it is evident that an overlap occurred in the thermal degradation of cellulose and lignin and the epoxy resin by the broad peak overlap between 350 and 400°C. This is in agreement with earlier works Yasmin and Daniel (2004) as well as Chun et al. (2013a). While Chun et al. (2013a) reported a degradation of the cellulose and lignin in coconut shell to have occurred between 350 and 400°C in coconut shell/Poly(lactic acid) eco-composites. Also, Yasmin and Daniel (2004) investigated the mechanical and thermal properties of graphite platelet/epoxy composites and reported a thermal degradation of epoxy resin to have started at about 366°C and ended at 450°C in 5% graphite filled epoxy composites. It is worth mentioning that the optimized brake pad contains 5% graphite. In the optimized seashell filled brake pad, a clear degradation peak is seen at about 427°C. This peak occurred at a lower temperature in the commercial (412°C) and coconut shell filled brake pad (400°C). This indicates that the thermal degradation of the epoxy in the seashell composites occurred at a higher temperature than in the coconut shell filled brake pad. Apart from the fact that the seashell is more thermally stable than the coconut shell, it is clear that incorporating seashell in an epoxy resin significantly improved its thermal stability. This is because seashell has been found to contain between 95-99% by weight of Calcium carbonate, CaCO<sub>3</sub> (Marin and Luquet, 2004). Hongwei et al. (2011) reported that incorporating nano calcium carbonate in epoxy improved the thermal stability of the resultant composites. The degradation of alumina in the brake pad is seen around 473.1°C in the seashell filled, 475.7°C in the coconut filled and 514.1 °C in the commercial brake pad samples. This is in line with the findings of Schwentenwein and Homa (2015) that investigated a new process for additive manufacturing of dense and strong ceramic objects and showed that the thermal degradation of alumina occurred between 400 and 500°C. Contrarily, Ramousse et al. (2001) reported that graphite in iron filled brake pads decomposed thermally between 688 and 850°C. While Schwentenwein and Homa (2015) examined the thermal decomposition of graphite in ceramic based composites, Ramousse et al. (2001) reported the thermal behaviour of graphite in iron-filled brake pads. The differences in the materials used may have accounted for the different degradation temperatures reported.

Another degradation event could be seen at about 900°C, which is attributed to the decomposition of CaCO<sub>3</sub> present in the seashell to CaO. Nurfatirah et al. (2015) reported that



at temperature of 815°C, a rapid weight loss occurred in seashell as CaCO<sub>3</sub> decomposes into CaO. However, this event could not be captured completely as the temperature range of the experiment is below this degradation event. Therefore, in this study, an environmentally friendly brake pad was produced with competitive thermal stability with the commercial brake pad. It is worth noting that these brake pads can be used in an automobile system whose braking temperature do not exceed 350°C for coconut shell-filled and 427°C seashell-filled brake pads.

### 3.2 Microstructure Analysis

The microstructure of impact-fractured surfaces of commercial and optimized samples observed at magnification on a scanning electron microscope (SEM) is shown in Figure 7.

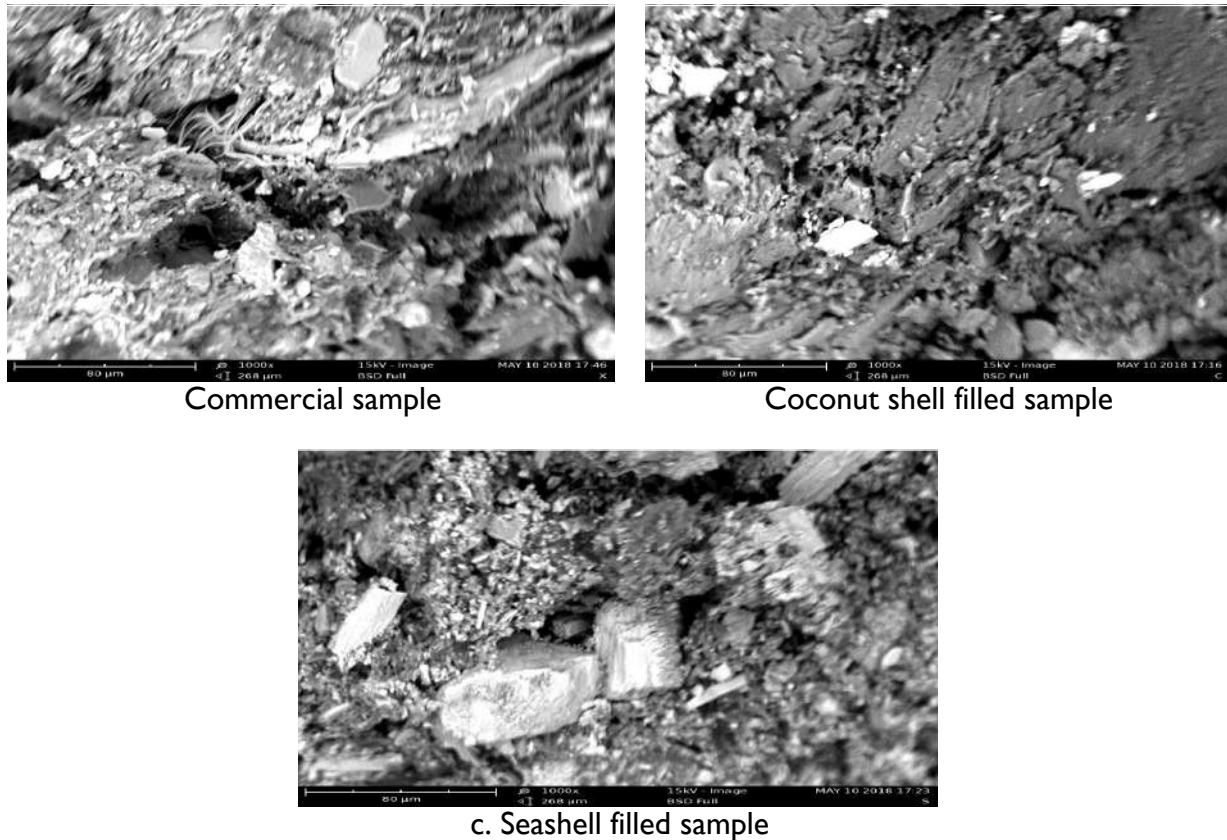


Figure 7: Microstructure of impact fractured Surfaces of brake pad pamples at 1000X Magnifications

The microstructures of the fractured surfaces shown in Figure 7 indicate the uniform distribution of various additives (seashell, coconut shell, graphite and alumina) in the friction materials. Overall observation indicates that the particles of the brake pad samples show good dispersion even though there are more traces of micro-voids in seashell-filled than in the commercial and coconut shell-filled samples. These differences in the level of voids present on each sample may be due to the variation in filler materials and process parameters used during production. Luka et al. (2016) studied the microstructure of a fiber/resin composite using SEM and found that the amount of voids in the composite was dependent on the fibre/resin content and processing conditions which in turn affect its performance. Also, it can be observed that all the fractured surfaces show basically brittle behaviour. Surfaces presented in Figure 7(a) shows the presence of asbestos fibres with patches of matrix adhering on the surfaces. In addition, Figure 7(b) revealed that there was more uniform distribution of the fillers in the resin, leading to better bonding between the epoxy resin and the filler in the coconut shell filled brake pad when compared to constituents of the seashell-filled samples as shown in Figure 7(c). Abutu et al. (2019) had reported better mechanical properties exhibited by these coconut shell-filled brake pads. Also, Plate I(c) revealed an agglomeration of constituent particles as two particles were observed to be contacting each other with patches of resin adhering to the surfaces. These results are in agreement with the previous work of Yawas et al. (2016), who studied the

microstructure of periwinkle shell filled brake pad and reported that the distribution of particles is influenced by good bonding properties of the binder and its constituent particles which in turn, lead to better inter- facial interaction.

#### 4. Conclusion

Seashell and coconut shell were used as asbestos-free fillers to produce brake pads. The properties of formulated multi-response optimized friction materials were investigated by examining their thermal degradation behaviour and microstructure. The following conclusions can be drawn:

From the grey relational analysis conducted, the seashell-filled brake pad should be produced using 14 MPa moulding pressure, MT of 160 °C moulding temperature, 12 minutes curing time and 1 hour heat treatment time while coconut shell-filled brake pad should be produce using 14 MPa moulding pressure, MT of 140 °C moulding temperature, 8 minutes curing time and 5 hours heat treatment time.

The microstructure of the developed coconut shell-filled brake pads gave a more uniform distribution of the fillers leading to better bonding and closer inter-packing distance compared to seashell-filled and commercial brake pad.

Thermal analysis shows that the commercial and seashell filled brake pad show better overall thermal resistance compared to coconut shell filled brake pads.

Finally, the thermal degradation profile revealed that the developed coconut shell brake pad can be applied in an automobile whose braking temperature do not exceed 350°C, while the seashell-filled brake pad can be applied in an automobile system whose braking temperature do not exceed 427°C. Overall, the commercial brake pad possessed a higher thermal stability as the components were not noticeably degraded at temperatures at which the coconut shell and the seashell filled brake pads showed appreciable degradation.

#### Acknowledgement

The authors are thankful to the management of Federal University of Technology Minna-Nigeria for the grant Senate/FUTMINNA/2015/03, allocated to this research.

Conflict of Interest: The authors declare that they have no conflict of interest in publishing this article.

#### References

- Abutu, J., Lawal, SA., Ndaliman, MB., Lafia-Araga, RA., Adedipe, O. and Choudhury IA. 2018. Effects of process parameters on the properties of brake pad developed from seashell as reinforcement material using grey relational analysis. *Engineering Science and Technology, an International Journal*, 21: 787–797.
- Abutu, J., Lawal, SA., Ndaliman, MB., Lafia-Araga, RA., Adedipe, O. and Choudhury, IA. 2019. Production and Characterization of Brake pad developed from Coconut shell reinforcement material using Central Composite Design. *SN Applied Sciences*, 1:18.
- Aigbodion, VS., Agunsoye, JO., Hassan, SB., Asume, F. and Akadike, U. 2010. Development of Asbestos-free Brake pad using Bagasse: *Tribology in Industry*, 32(1): 12-18.
- Andrzej, KB., Abdullah, AM. and Jürgen, V. 2010. Barley husk and coconut shell reinforced polypropylene composites: The effect of fibre physical, chemical and surface properties, *Composites Science and Technology*, 70: 840–846.
- Askeland, DR. 1985. *The Science and Engineering of Materials*. Massachusetts, PWS Publishers: U.S.A.
- Bhaskar, J. and Vinay, KS. 2013. Physical and Mechanical Properties of Coconut Shell Particles Filled-Epoxy Composite. *Journal of Materials and Environmental Science*, 4(2): 227-232.
- Chemiplastica 2010. *Thermoset Processing Manual Compression Molding*, Retrieved from, <http://www.chemiplastica.com/pdf/compression-molding-guidelines.pdf>, accessed on 5 August, 2015.

- Chen, KS., Yeh, RZ. and Wu, CH. 1997. Kinetics of Thermal Decomposition of Epoxy Resin in Nitrogen-Oxygen Atmosphere. *Journal of Environmental Engineering*, 123(10): 1041-1046.
- Cho, M., Kim, D. and Kim SJ. 2005. Effects of ingredients on tribological characteristics of a brake pad: An experimental case study. *Wear*, 258(11-12): 1682-1687.
- Chun, KS., Husseinsyah, S. and Osman, H. 2013a. Properties of Coconut Shell Powder-Filled Polylactic Acid Eco composites: Effect of Maleic Acid. *Polymer Engineering and Science*, 53(5): 1009-1116.
- Chun, KS., Husseinsyah, S. and Azizi, FN. 2013b. Characterization and Properties of Recycled Polypropylene/Coconut Shell Powder Composites: Effect of Sodium Dodecyl Sulfate Modification. *Polymer-Plastics Technology and Engineering*, 52(3): 287–294.
- Cyras, VP., Iannace, S., Kenny JM., and Vazquez, A. 2001. Relationship between processing and properties of biodegradable composites based on PCL/starch matrix and Sisal fibers. *Polymer Composites*, 22(1): 104-110.
- Dagwa, IM., and Ibadode, AO. 2006. Determination of Optimum Manufacturing conditions for Abestos-free Brake Pad using Taguchi optimization Method. *Nigeria Journal of Engineering Research and Development*, 5(4): 1-8.
- Hongwei, H., Kaixi, L., Jian, W., Guohua, S., Yanqiu, L. and Jianlong, W. 2011. Study on thermal and mechanical properties of nano-calcium carbonate/epoxy composites. *Materials and Design*, 32(8-9): 4521–4527.
- Ikpambese, KK., Gundu, DT. and Tuleu, LT. 2014. Evaluation of palm kernel fibers (PKFs) for production of asbestos-free automotive brake pads. *Journal of King Saud University – Engineering Sciences*, 28(1): 110–118.
- Islam, KN., Bakar, MZBA., Ali, ME., Hussein, MZB., Noordin, MM., Loqman, MY. and Hashim, U. 2013. A novel method for the synthesis of calcium carbonate (aragonite) nanoparticles from cockle shells. *Powder Technology*, 235: 70–75.
- Jang, H., Basch, RH., Ko, K., Kim, SJ. and Fash, JW. 2004. The Effect of Metal Fibers on the Friction Performance of Automotive Brake Friction Materials. *Journal of Wear*, 256(3-4): 406-414.
- Lawal, SA., Ugwuoke, IC., Abutu, J., Lafia-Araga, RA., Dagwa, IM. and Karim, I. 2016. Rubber Scrap as Filled Material in the Production of Environmentally Friendly Brake Pad. *Module in Materials Science and Materials Engineering*, Elsevier Oxford., pp.1-10.
- Luca, DL., Aurelio, M., Paolo, B., Stefania, G., Fabrizio, M. and Marco, R. 2016. Detection of voids in Carbon/Epoxy Laminates and their influence on mechanical properties. *Polymers and Polymer Composites*, 25(5): 371-380.
- Marin, F. and Luquet, G. 2004. Molluscan shell proteins. *Comptes Rendus Palevol*, 3(6-7): 469-492.
- Mustakimah, M., Suzana, Y. and Saikat, M. 2012. Decomposition Study of Calcium Carbonate in Cockle Shell. *Journal of Engineering Science and Technology*, 7(1): 1–10.
- Mutlu, I., Eidogan, O. and Findik, F. 2005. Production of ceramic additive automotive brake pad and investigation of its braking characteristics. *International journal of Tribology*, 57(2): 84-92.
- Natarajan, MP., Rajmohan, B. and Devarajulu, S. 2012. Effect of Ingredients on Mechanical and Tribological Characteristics of Different Brake Liner Materials. *International Journal of Mechanical Engineering and Robotic Research*, 1(2): 135-157.
- Nurfatihah, N., Zainab, H., Othman, H., Farizul, HK. and Rozaini, A. 2015. Effect of Temperature in Calcination Process of Seashells. *Malaysian Journal of Analytical Sciences*, 19(1): 65–70.
- Ole-Von, U., Staffan, S., Reed, D. and Michael B. 2005. Antimony in brake pads-a carcinogenic component? *Journal of Cleaner Production*, 13(1): 19–31.
- Ramousse, S., Høj, JW. and Sørensen, OT. 2001. Thermal Characterization of Brake Pads. *Journal of Thermal Analysis and Calorimetry*, 64: 933-943.

Ruzaidi, CM., Mustafa, AB., Shamsul, JB., Alida, A. and Kamarudin, H. 2011. Morphology and Wear Properties of Palm Ash and PCB Waste Brake Pad. International Conference on Asia Agriculture and Animal IPCBEE held in Singapore, 2-3 July 2011, Proceedings pp. 145-149.

Schwentenwein, M. and Homa, J. 2015. Additive Manufacturing of Dense Alumina Ceramics. International Journal of Applied Ceramic Technology, 12(1): 1-7.

Talib, RJ., Mohmad, SS. and Ramlan, K. 2012. Selection of best formulation for semi-metallic brake friction materials development. Katsuyoshi Kondoh (Ed), Powder Metallurgy, pp. 1-13, InTech Publisher, Shanghai, China.

Tanaka, K., Ueda, S. and Noguchi, N. 1973. Fundamental studies on the brake friction of resin-based friction materials. Wear, 23(3): 349-365.

Yasmin, A. and Daniel, IM. 2004. Mechanical and thermal properties of graphite platelet/epoxy composites. Polymer, 45(24): 8211-8219.

Yawas, DS., Aku, SY. and Amaren, SG. 2016. Morphology and properties of periwinkle shell asbestos-free brake pad. Journal of King Saud University- Engineering Sciences, 28(1): 103-109.

Yiyo, K., Taho, Y. and Guan, WH. 2008. The use of a grey-based Taguchi method for optimizing multi-response simulation problems. Engineering Optimization, 40(6): 517-528.

Zaharudin, A.M., Berhan, M.N., and Talib, R.J. 2011. The Effect of Phenolic Resin, Rubber, Calcium Carbonate and Graphite on Tribological Characteristic of Semi-Metallic Brake. AIP Conference Proceedings held in Antalya, Turkey, 12-15 May 2011, 1400: 274-279.